

Desferrioxamine-mediated Iron Uptake in *Saccharomyces cerevisiae*

EVIDENCE FOR TWO PATHWAYS OF IRON UPTAKE*

(Received for publication, December 21, 1999, and in revised form, January 12, 2000)

Cheol-Won Yun^{‡§}, Tracy Ferea^{§¶}, Jared Rashford[‡], Orly Ardon^{¶*}, Patrick O. Brown^{‡‡},
David Botstein[¶], Jerry Kaplan^{§§}, and Caroline C. Philpott^{¶¶}From the [‡]Liver Diseases Section, NIDDK, National Institutes of Health, Bethesda, Maryland 20892-1800, the [¶]Department of Genetics, Stanford University School of Medicine, Stanford, California 94305-5120, the ^{||}Department of Pathology, School of Medicine, University of Utah, Salt Lake City, Utah 84132, and the ^{‡‡}Department of Biochemistry, Stanford University School of Medicine, Howard Hughes Medical Institute, Stanford, California 94305-5428

In the yeast *Saccharomyces cerevisiae*, uptake of iron is largely regulated by the transcription factor Aft1. cDNA microarrays were used to identify new iron and AFT1-regulated genes. Four homologous genes regulated as part of the AFT1-regulon (*ARN1–4*) were predicted to encode members of a subfamily of the major facilitator superfamily of transporters. These genes were predicted to encode proteins with 14 membrane spanning domains and were from 26 to 53% identical at the amino acid level. *ARN3* is identical to *SIT1*, which is reported to encode a ferrioxamine B permease. Deletion of *ARN3* did not prevent yeast from using ferrioxamine B as an iron source; however, deletion of *ARN3* and *FET3*, a component of the high affinity ferrous iron transport system, did prevent uptake of ferrioxamine-bound iron and growth on ferrioxamine as an iron source. The siderophore-mediated transport system and the high affinity ferrous iron transport system were localized to separate cellular compartments. Epitope-tagged Arn3p was expressed in intracellular vesicles that co-sediment with the endosomal protein Pep12. In contrast, Fet3p was expressed on the plasma membrane and was digested by extracellular proteases. These data indicate that *S. cerevisiae* has two pathways for ferrioxamine-mediated iron uptake, one occurring at the plasma membrane and the other occurring in an intracellular compartment.

Iron is an essential nutrient for virtually every organism, and it is required for many cellular processes. Although iron is the second most abundant metal in the earth's crust, it is not readily bioavailable, because iron is largely present as poorly soluble complexes of ferric hydroxide. Therefore, organisms from microbes to man have developed mechanisms for obtaining iron from the environment. The budding yeast *Saccharomyces cerevisiae* has two characterized systems of elemental iron uptake, a low affinity system encoded by *FET4* (1) and a high affinity system encoded by *FET3* and *FTR1* (2, 3). Both transport systems require the action of surface reductases

(*FRE1* and *FRE2*) to reduce Fe(III) to the more soluble Fe(II) (4, 5).

Reduction followed by transport of elemental iron is only one of the strategies that organisms use to accumulate iron. Most bacteria and fungi synthesize and secrete siderophores, low molecular weight compounds that specifically bind ferric iron. Siderophores bind ferric iron with high affinity, and the siderophore-iron complex can be captured by specific cellular transport systems. Most bacteria and fungi synthesize at least one type of siderophore but may express transporters specific to that siderophore as well as to siderophores secreted by other species (6). Prokaryotic mechanisms of siderophore uptake are well described (7), but much less is known about eukaryotic siderophore utilization (8). Although neither budding nor fission yeast secrete siderophores, they are capable of taking up siderophore-bound iron (9, 10).

The high affinity transport system for elemental iron in *S. cerevisiae* is under the control of the iron-dependent transcriptional regulator, Aft1p (11, 12). Through the use of cDNA microarrays representing virtually the entire genome of *S. cerevisiae*, we have identified genes that are regulated according to iron availability and Aft1p expression. Here, we report that four homologous members of the major facilitator superfamily of transporters are transcriptionally regulated by Aft1p. One of these, *ARN3*, is identical to *SIT1*, a gene reported to have a role in ferrioxamine B-mediated iron transport (13). Ferrioxamine B is a hydroxamate-type siderophore that is synthesized and secreted in its iron-free form, desferrioxamine B (DFO)¹ by several species of actinomycetes (14). Here we demonstrate that both *ARN3* and *FET3* can facilitate the uptake of DFO-bound iron (DFO-Fe). We further demonstrate that although Fet3p is localized to the cell surface, Arn3p is found predominantly in intracellular, post-Golgi vesicles.

MATERIALS AND METHODS

Yeast Strains, Plasmids, and Media—Strain DBY7286 (*MATa ura3 GAL*) and congenic *aft1* mutants were used for cDNA microarray analysis and were constructed as described (15). All other strains were constructed in YPH499 *MATa ura3-52 lys2-801(amber) ade2-101(ochre) trp1-Δ63 his3-Δ200 leu2-Δ1* (Yeast Genetic Stock Center, Berkeley, CA). PCR-mediated gene disruption was used to generate deletions of the *ARN* genes (16). The following primers were used to amplify the HISG-URA3-HISG cassette from the plasmid pMPY-ZAP: for *ARN1*, 5'-GGGAATGGAACACGAGTTGAATCCTGAGACTCATAACGATTC-CAACTCCGACTCCTACTATAGGGCGAATTGG-3' and 5'-CGTGTCCGACATATTCGCCATCCTCGATGTATTCCACAGCAACAGTATCAGTCTAAAGGGAACAAAAGCT-3'; for *ARN2*, 5'-GTAATGAACTGATGGT-TGATGAAAAGAGGATGACGATTCGTCGCCAGAGATGCTCACTA-

* The costs of publication of this article were defrayed in part by the payment of page charges. This article must therefore be hereby marked "advertisement" in accordance with 18 U.S.C. Section 1734 solely to indicate this fact.

§ These authors contributed equally to this work.

¶ Supported by Post-doctoral Award FI274-98 from the United States-Israel Binational Agricultural Research and Development Fund.

§§ Supported by Grant NIDDK-305340 from the National Institutes of Health.

¶¶ To whom correspondence should be addressed. E-mail: carolinep@intra.niddk.nih.gov.

¹ The abbreviations used are: DFO, desferrioxamine B; DFO-Fe, DFO-bound iron; PCR, polymerase chain reaction; HA, hemagglutinin; kb, kilobase(s); BPS, bathophenanthroline sulfonate.

TAGGGCGAATTGG-3' and 5'-CCAGTCATTGATAGGATCATCTTCC-TTGGTTTGGACATATTCTCTGTGTCAGGTAACCTAAAGGGAACAAA-GCTGG-3'; for ARN3, 5'-GACCCTGGTATTGCTAATCATACCTCCCGAGGAATTTGAAGAGGTTGTCTCACTATAGGGCGAATTGG-3' and 5'-CCAAACCTAGATACATAAAAATCTTTTGAACATAGCGGTAA-GACATGACTAAAGCCTAAAGGGAACAAAAGCT-3'; and for ARN4, 5'-TGACAATTTAGACGATAAAAGCACTGTCTGCTACAGCGAAAAG-ACAGATAGCCTCACTATAGGGCGAATTGG-3' and 5'-TATCCAATT-ACAGACGAGCCATGATTGTTGTTGATTTGAGCTTCTCTTCT-AAAGGGAACAAAAGCT-3'. Deletions were confirmed by PCR and 5-fluoroorotic acid-resistant clones were selected. Construction of double, triple, and quadruple *ARN* deletion mutants was performed by repeated PCR-based gene disruption and by mating and sporulating single deletion strains. Deletion of *FET3* was performed as described (3). The strain *YPH499 FET3-HA FTR1-myc*, which constitutively over-expresses integrated copies of HA-tagged *FET3* and *myc*-tagged *FTR1* under the control of the phosphoglycerate kinase promoter, was constructed as described (17). The ARN3-HA strain, which expresses a triple copy of the HA epitope fused to the carboxyl terminus of Arn3p, was constructed by PCR epitope tagging as described using the plasmid pMPY-3xHA (18) and the following primers: 5'-TTGAAAAATAAATT-CTTTACGCACTTTACAAGCAGTAAAGATAGGAAAGATGAACAAAA-GCTGGAGCTCCAC-3' and 5'-ACTATGTAGTAGCTATATGTGCATG-TATGAAATTATTTGGGTGAGATAAATACTATAGGGCGAATTGGGTA-CC-3'. Integration of the HA epitope was confirmed by PCR and by Western blotting. The plasmid pARN3-HA was constructed by extracting genomic DNA from the ARN3-HA strain and digesting it with *NruI* and *PstI*. After electrophoresis, DNA fragments from 3.0 to 5.0 kb were extracted (GELase, Epicentre Technologies), ligated into *PstI*- and *SmaI*-digested pRS415 (Stratagene), and used to transform *Escherichia coli* DH5- α . Clones were screened by colony hybridization using a 0.46-kb *EcoRV* fragment of *ARN3*, and positive clones were further analyzed by restriction mapping. Plasmid-encoded expression of Arn3p-HA was confirmed by Western blotting. Rich medium (YPD) and defined medium (SD) were prepared as described (19). Defined iron media were prepared as described (15).

Microarrays—Strains were cultured in the exponential phase of growth for more than five generations in either SD complete medium or defined iron media with 20 μ M (low iron), 100 μ M (optimal iron), or 500 μ M (high iron) added ferrous ammonium sulfate. Low iron and high iron culture conditions were selected in which the rate of growth was moderately but not severely (< 2-fold difference when compared with the optimal iron condition) affected by iron limitation or excess (data not shown). Cultures were harvested at a uniform cell density of 1×10^7 cells/ml. Total RNA was extracted using Trizol (Life Technologies, Inc.) according to the manufacturer's instructions. Probe preparation, microarray production, hybridization, and data analysis were performed as described (20, 21).

Northern Analysis—Yeast were grown to mid-log phase in SD medium or defined iron media containing the indicated amount of ferrous iron. Total RNA was extracted using Trizol (Life Technologies, Inc.), and Northern blot analysis was performed as described (11). Probes for the *ARN* genes were as follows: for *ARN1*, a 1.15-kb *HincII* fragment; for *ARN2*, a 0.8-kb *NdeI* fragment; for *ARN3*, a 0.46-kb *EcoRV* fragment; and for *ARN4*, a 0.7-kb *AluNI* fragment. Restriction fragments were isolated from a PCR-amplified product corresponding to the open reading frame of each *ARN* gene.

Desferrioxamine B Plate Assay and Iron Uptake Assay—For the plate assay, modified synthetic complete media were used in which copper and iron were omitted and 1 μ M copper sulfate and 100 μ M bathophenanthroline sulfonate (BPS, a ferrous iron chelator that is not taken up by yeast) were added. Trace amounts of iron are supplied by agar (Difco). Desferrioxamine B+ plates also included 100 μ M of the mesylate derivative of DFO (Desferal, Sigma). Yeast strains were grown for 24 h on plates of defined-iron media (approximately 10 μ M iron) to deplete intracellular iron stores. Cells were then suspended in water at 2×10^6 cells/ml, plated in serial 10-fold dilutions, and incubated at 30 °C for 3 days prior to imaging. Ferrous iron uptake assays were performed as described using 1 μ M ^{55}Fe , except that washes were omitted and cells were spun through a column of 10% bovine serum albumin before scintillation counting (22). For DFO uptake assays, 1 μ M ferric ^{55}Fe and 1 μ M DFO were used.

Immunofluorescence, External Protease Digestion, and Western Blotting—Strains were grown to mid-log phase in defined iron media containing 10 μ M ferrous ammonium sulfate to induce the expression of Arn3. Cells were washed and prepared for immunofluorescence microscopy as described (3). Primary antibody was affinity purified HA.11 (BAbCo) at 1:500, and secondary antibody was Cy3-conjugated poly-

clonal anti-mouse IgG from donkey (Jackson Immunoresearch) at 1:500. Cells were imaged on a Nikon photomicroscope equipped with 100 \times /1.3NA objective with Nomarski optics. Images were acquired using IP Labs software and a CCD camera (Princeton Instruments). Susceptibility to external protease in living cells was performed essentially as described (23). Washed cells were resuspended at 2×10^7 cells/ml and incubated for 1 h with 2 mg/ml proteinase K or for 20 min with 0.7 mg/ml Pronase prior to lysis. Cells were lysed on ice in 1.85 M NaOH and 1% 2-mercaptoethanol for 10 min followed by precipitation on ice in 25% trichloroacetic acid for 30 min. Precipitates were resuspended in SDS sample buffer containing 0.1 M Tris base before SDS-polyacrylamide gel electrophoresis. Western blotting was performed using a 1:2000 dilution of HA.11 ascites (BAbCo). The secondary antibody consisted of anti-mouse IgG conjugated to horseradish peroxidase (Amersham Pharmacia Biotech) diluted 1:3000 and was detected by chemiluminescence (Pierce), according to the manufacturer's protocols.

Membrane Fractionation and Western Blotting—Cell cultures were grown to an A_{600} of 1.0 in iron limiting conditions (CM + BPS 40 μ M). Briefly, cells were washed, spheroplasted, and processed as described previously (24). Membranes were applied to an 0–25% Iodixanol (Life Technologies) gradient, which was centrifuged at 10,000 $\times g$ for 2 h and then fractionated. Samples from each fraction were loaded on a 12% SDS-polyacrylamide gel electrophoresis, which was transferred to a nitrocellulose membrane. The localization of fractions containing mitochondria, vacuoles, endoplasmic reticulum, and late endosomes was determined by Western analysis using antibodies against mitochondrial porin (Molecular Probes), carboxypeptidase Y (Molecular Probes), dolichol phosphate mannose synthetase (Molecular Probes), and Pep12 (a gift of Dr. Scott Emr, UCSD), respectively. The refractive index of each fraction was determined by a Bausch and Lomb refractometer.

RESULTS

Identification and Sequence Analysis of *ARN* Genes—cDNA microarray analysis was performed to examine the yeast genome for new genes involved in iron metabolism (20, 21). This technique allows each gene in the yeast genome to be analyzed for differences in mRNA transcript levels when a pair of strains or culture conditions is compared. We compared mRNA obtained from yeast expressing a constitutively active allele of *AFT1*, *AFT1-1^{up}*, and a congenic strain with the *AFT1* gene deleted, *aft1 Δ* . Expression of *AFT1-1^{up}* results in high levels of transcription of the genes of high affinity iron uptake, and a failure of these genes to be repressed by exogenous iron (11). Conversely, in *aft1 Δ* strains, transcription of genes involved in high affinity iron uptake is greatly reduced, even under conditions of iron depletion. Genes were identified in microarrays that were more highly expressed in an *AFT1-1^{up}* strain than in the *aft1 Δ* strain. Similar comparisons were made between *AFT1-1^{up}* and wild type strains and between wild type strains grown in reduced amounts of iron or increased amounts of iron (Fig. 1A). Four of the genes identified in this fashion, YHL040C, YHL047C, YEL065W, and YOL158C, were chosen for further study. These genes are predicted to encode highly homologous members of a subfamily of the major facilitator superfamily of transporters (25–27). Two other members of this subfamily, YKR106W and YCL073C, were not differentially expressed in the arrays. The DNA regions upstream of the open reading frames of YHL040C, YHL047C, YEL065W, and YOL158C were analyzed, and all were found to contain *AFT1* consensus binding sites (12) within 500 nucleotides of the start codon, as would be expected for *AFT1*-regulated genes (Fig. 1B). These genes were designated *ARN1*, 2, 3, and 4, respectively.

A comparison of the predicted amino acid sequences of these genes (Fig. 1C) revealed that the overall sequence identity ranges from 26 to 53%, with *ARN1* and *ARN2* showing the greatest sequence identity and *ARN4* the least. The predicted proteins have 14 membrane-spanning domains, and both the amino and carboxyl termini are predicted to be cytosolic.

Regulation of *ARN* Expression by Iron and *AFT1*—To confirm the results of the cDNA microarrays, iron- and *AFT1*-de-

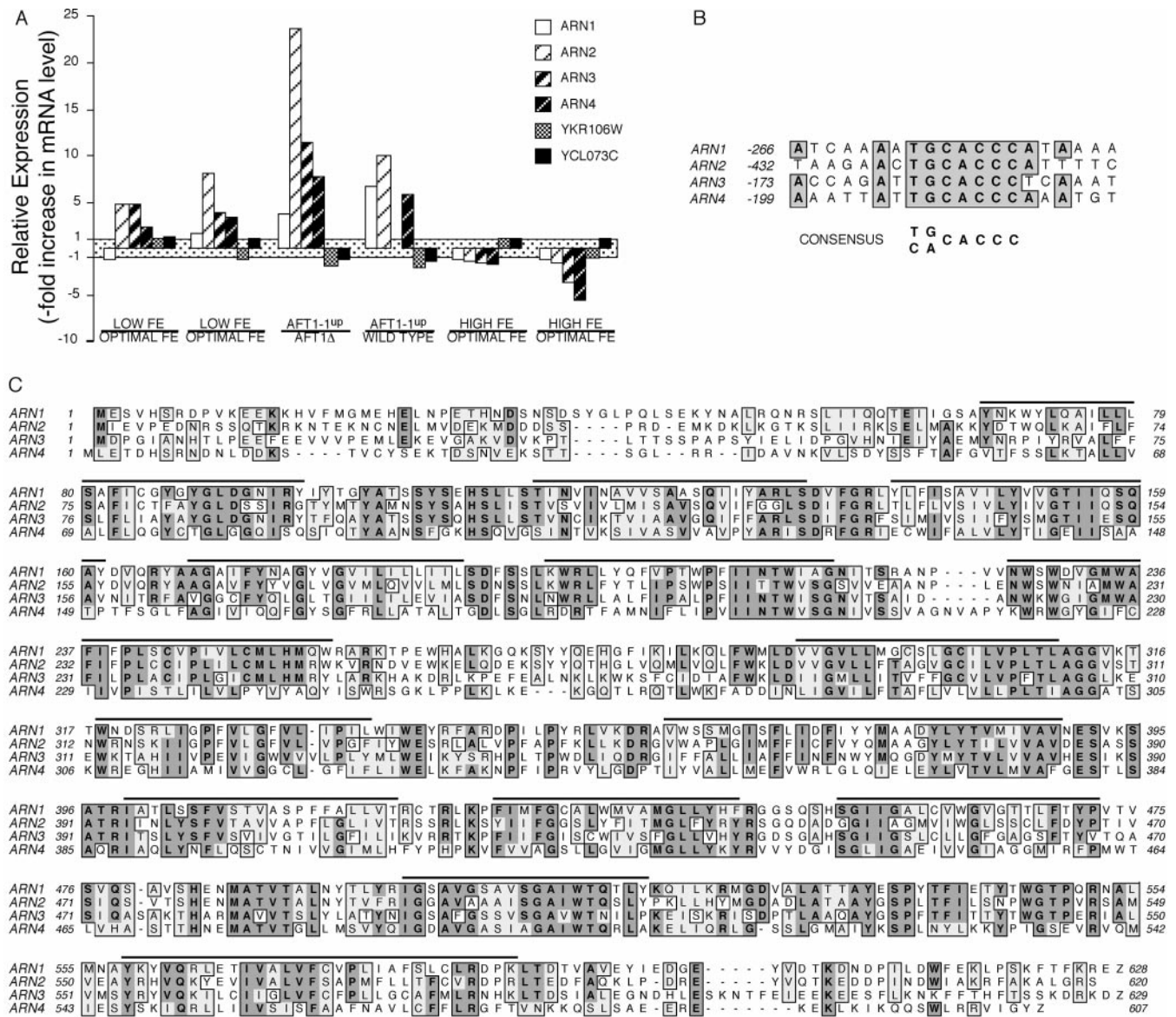


FIG. 1. Identification of *ARN1*, *ARN2*, *ARN3*, and *ARN4*. *A*, relative mRNA levels of *ARN* genes, *YKR106W*, and *YCL073C* in cDNA microarrays. Each array is a pairwise comparison of RNA obtained from two different culture conditions. *Bar height* indicates the ratio of the mRNA levels for a single gene in an array. Positive values >1 indicate the gene was more highly expressed in the top condition of the pair, and negative values <1 indicate the gene was more highly expressed in the bottom condition of the pair. Results from individual arrays are shown. *B*, *Aft1* consensus binding sites. Nucleotide sequences upstream of the open reading frames were scanned for potential *Aft1* binding sites in accordance with the published consensus sequence. *Boxed* and *shaded areas* indicate sequence identity. *C*, sequence alignment of *ARN1*, *ARN2*, *ARN3*, and *ARN4*. *Boxed areas* indicate regions of amino acid similarity, and *darkly shaded areas* indicate amino acid identity. *Bars* indicate potential membrane spanning domains as predicted by TMpred.

pendent regulation of the mRNA levels of *ARN1–4* were examined by Northern blot analysis (Fig. 2). The transcript profile for all four *ARN* genes was found to be similar. In the wild type strain, *ARN* transcript levels were high when cells were grown in iron-limited media and greatly reduced when higher concentrations of iron were present (lanes 1–7). The effects of expression of different *AFT1* alleles on *ARN* transcript levels was examined in cells grown in iron replete media (lanes 8–10). In these media, *AFT1*-dependent transcription is low, as are high affinity iron uptake and surface reductase activities (data not shown). *ARN* transcript levels were low in both *AFT1* and *aft1Δ* strains (lanes 8 and 9). In contrast, *ARN* transcripts were abundant in an *AFT1-1^{up}* strain (lane 10). These results suggest that transcription of *ARN1–4* is a direct consequence of *AFT1* activation and is not a secondary result of iron deprivation.

The Role of *ARN3* and *FET3* in Desferrioxamine-mediated

Growth and Iron Uptake—*ARN3* was reported to be involved in the transport of the hydroxamate siderophore DFO-Fe (13). To determine the genetic requirements for growth with DFO-Fe as an iron source, we examined the capacity of DFO-Fe to supply iron to yeast strains with deletions in *ARN* genes (Fig. 3). Both *ARN⁺* and *arnΔ* strains showed decreased growth on iron-limited media. A deletion in the high affinity iron transport system (*fet3Δ*; Fig. 3B) resulted in no detectable growth in iron-limited medium. Both *ARN⁺* and *arn*-deleted strains grew well in iron-limited medium when DFO-Fe was added as an iron source (Fig. 3C). Strains with a functional high affinity iron transport system also were able to grow in DFO-Fe medium when the *ARN* genes were deleted in combination (pairs, triplets, or quadruplicate; data not shown). Deletion of *FET3* had no effect on growth in DFO-Fe media in an *ARN⁺* strain or when *ARN1*, 2, or 4 was deleted (Fig. 3D). Deletion of *ARN3* in a *fet3Δ* strain, however, completely prevented growth on DFO-

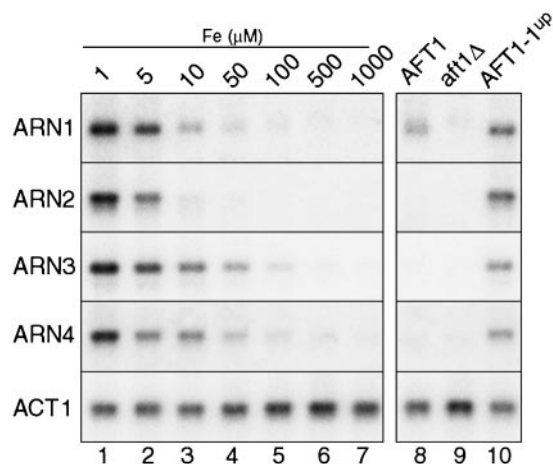


FIG. 2. Iron- and *AFT1*-dependent expression of *ARN1*, *ARN2*, *ARN3*, and *ARN4*. Total RNA was isolated from YHP499 (*AFT1*) in the exponential phase of growth after culture in defined-iron media (lanes 1–7) containing the indicated amounts of ferrous iron and from congenic strains YHP499, CPY101 (*aft1* Δ), and CPY121 (*AFT1*-1^{up}) after growth in SD complete medium (lanes 8–10). Northern blot analysis was performed with sequential hybridization of the indicated probes.

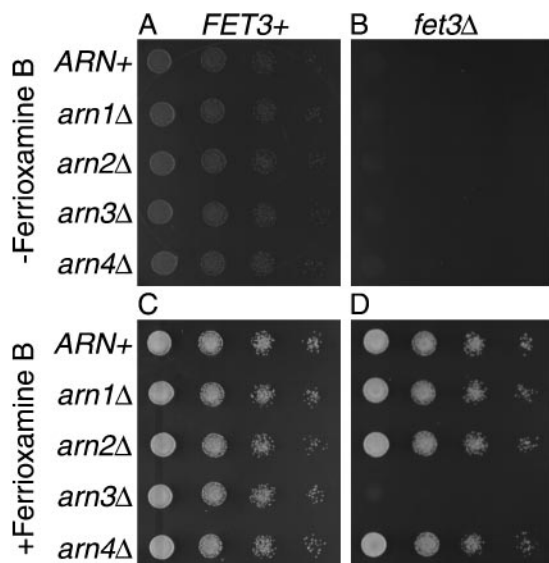


FIG. 3. Failure of DFO-Fe to sustain growth in yeast deleted for *FET3* and *ARN3*. Congenic strains of the indicated genotype were plated in serial dilutions on synthetic iron-poor media containing 100 μM BPS (–*Ferrioxamine B*) or 100 μM BPS and 100 μM desferrioxamine (+*Ferrioxamine B*). Plates were incubated at 30 °C for 3 days.

Fe. Expression of *ARN3* by either a high or low copy number plasmid completely restored growth on DFO-Fe medium, whereas expression of *ARN1* from a high copy number plasmid did not complement the growth deficit (data not shown). These data suggest the existence of two independent systems for the transport of iron bound to DFO: one system that requires the high affinity iron transporter composed of *FET3* and *FTR1* and a second system that requires *ARN3*.

We measured the cellular uptake of iron as Fe(II) and as DFO-Fe(III) in *ARN* deletion strains (Fig. 4). Deletion of individual *ARN* genes had no effect on the rate of Fe(II) uptake in strains expressing *FET3* (Fig. 4A). In contrast, the rate of uptake of iron from DFO-Fe was similar in wild type cells and Δ *fet3* cells but was reduced 4-fold in *arn3* Δ cells and was virtually undetectable in an *arn3* Δ *fet3* Δ strain (Fig. 4B). Again, these data indicate that uptake of DFO-bound iron is dependent on either *FET3* or *ARN3*.

Localization of ARN3 to Intracellular Vesicles—Transport of

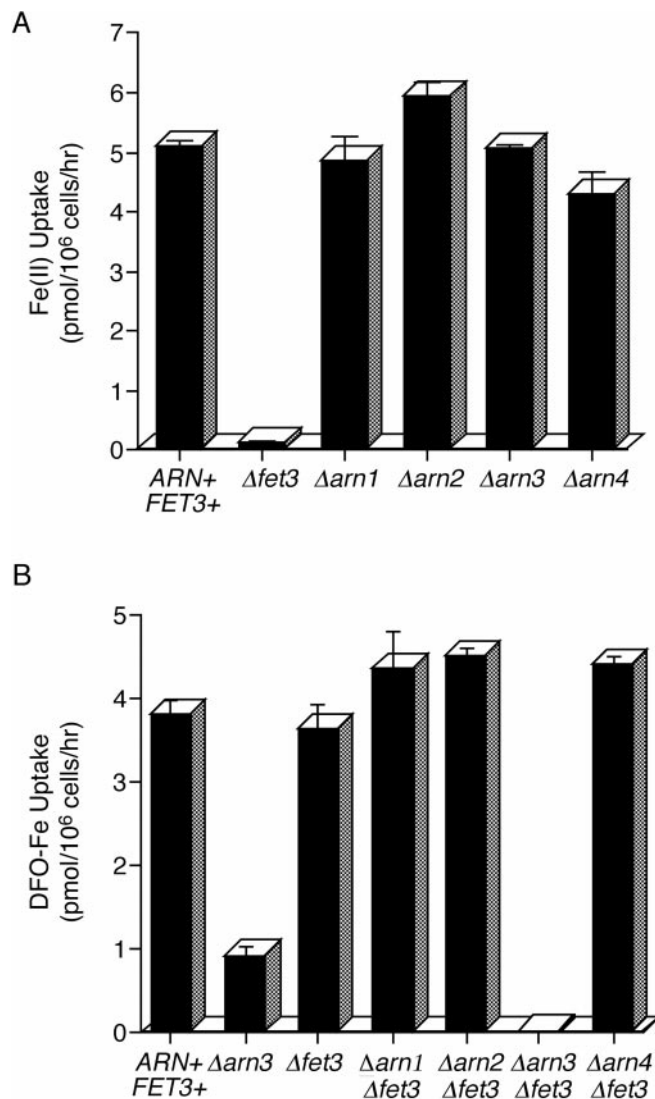


FIG. 4. Requirement of either *FET3* or *ARN3* for DFO-⁵⁵Fe uptake. A, intact ferrous iron uptake system in *ARN* mutants. Congenic strains of the indicated genotype were grown in defined-iron medium with 10 μM ferrous iron and assayed for the uptake of ⁵⁵Fe(II) as described under “Experimental Procedures.” B, specific requirement for *ARN3* in non-*FET3*-mediated DFO-Fe uptake. Congenic strains of the indicated genotype were grown in YPD medium and assayed for the uptake of DFO-⁵⁵Fe. Assays were performed in duplicate, and the experiment was replicated three times. Data from a representative experiment are shown.

iron through the high affinity system occurs at the plasma membrane. Both components of the high affinity iron transport system, the permease (*Ftr1p*) and oxidase (*Fet3p*), have been localized to the plasma membrane by immunological methods (3, 28, 29). We performed indirect immunofluorescence to determine whether DFO-mediated iron transport occurs at the plasma membrane. Strains were constructed in which the chromosomal copy of *ARN3* carried a triple-copy of the HA epitope at the carboxyl terminus or which contained an integrated copy of an overexpression cassette of HA-tagged *FET3* and Myc epitope-tagged *FTR1* (Fig. 5). We confirmed that the epitope-tagged version of *ARN3* was functional by cloning the HA-tagged allele into a low copy number plasmid and observing complementation of both the growth defect on DFO and the uptake defect of DFO-Fe iron of an Δ *arn3* Δ *fet3* strain (data not shown). When the strains were grown in media containing limiting amounts of iron to induce *ARN3* expression, HA-tagged *Arn3p* was not detected on the plasma membrane but

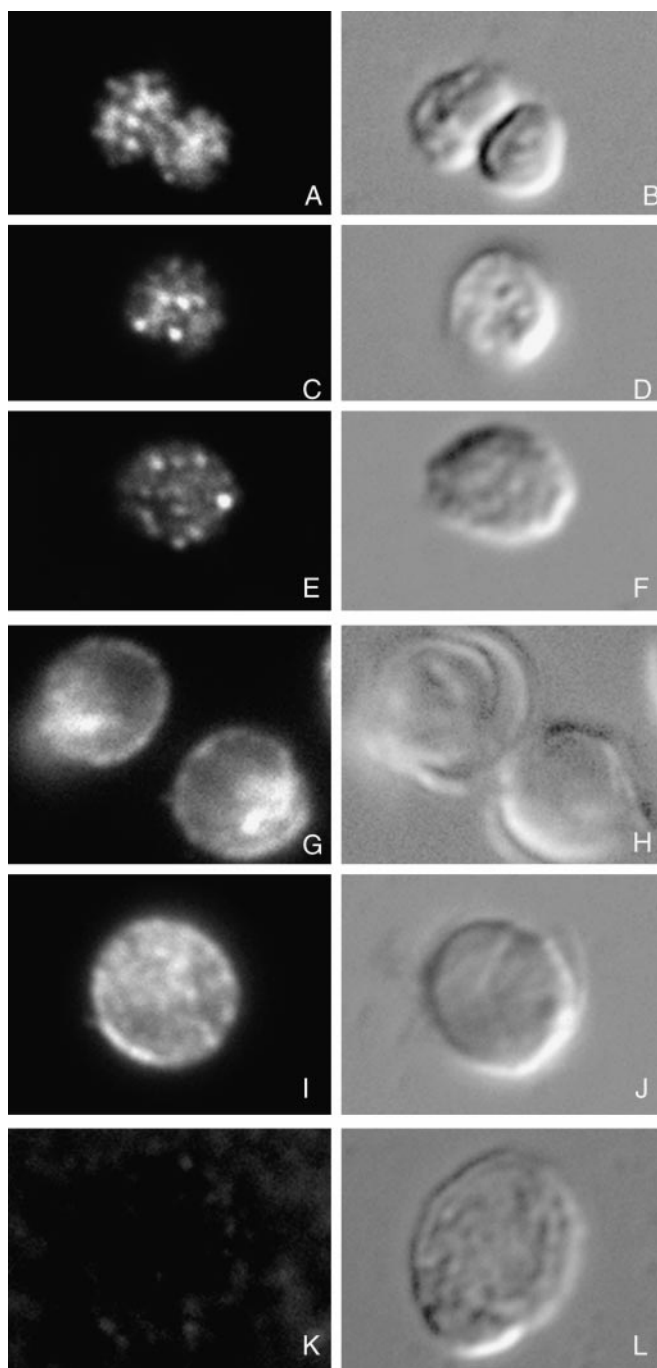


FIG. 5. **Localization of Arn3 to intracellular vesicles.** Indirect immunofluorescence microscopy was performed on Arn3p-HA (A–F) and Fet3p-HA (G–I) expressing cells and on the untagged parent strain (K and L). HA.11 was used as primary antibody, Cy3-conjugated donkey anti-mouse was the secondary antibody. Images are in pairs with fluorescence on the left and DIC on the right.

rather in multiple, small, intracellular vesicles that tended to cluster at the periphery of the cell (Fig. 5, A–E). In contrast, HA-tagged Fet3p was detected predominantly on the plasma membrane, although some intracellular signal was detected as well (Fig. 5, G–I).

The cellular localization of Arn3p may have been altered by fixation and antibody binding procedures. Unfortunately, when green fluorescent protein was fused to either the amino- or carboxyl terminus of ARN3, the cleaved green fluorescent protein moiety appeared in the lumen of the vacuole, thus precluding the visualization of Arn3p in living cells (data not shown). To determine whether Arn3p was expressed on the plasma

membrane, we treated intact cells with extracellular proteases and analyzed lysates by Western blotting (Fig. 6). As expected, Fet3p-HA was sensitive to extracellular proteases and was detected as an approximately 16-kDa fragment after protease digestion (lanes 9 and 10). In contrast, Arn3p-HA was highly resistant to extracellular protease (lanes 5 and 6) but was completely degraded by protease in the presence of detergent (lane 8). The susceptibility of Arn3p-HA to external protease was not altered when cells were grown in the presence of DFO, suggesting that Arn3p is not recruited to the plasma membrane in the presence of its transport substrate. These data confirm that the majority of Fet3p is localized to the plasma membrane in living cells and suggests that the majority of Arn3p is sequestered in an intracellular compartment.

To characterize the Arn3p-containing intracellular vesicles, we fractionated Arn3p-HA-expressing cells and separated subcellular organelles by density gradient centrifugation. Western blot analysis demonstrated that Arn3p-HA was not associated with vacuoles (Cpy1), endoplasmic reticulum (Dpm1), or mitochondria (Fig. 7, *Porin*). The distribution of Arn3p, however, was coincident with that of Pep12p, a protein enriched in late endosomes/prevacuoles (30). These results confirm the immunofluorescence studies and indicate that Arn3p is localized primarily in intracellular vesicles.

DISCUSSION

We have used microarray technology to identify four highly homologous genes that are regulated by the iron-dependent transcription factor Aft1p. Although one of the genes, *ARN3* (*SIT1*), was previously reported to exhibit an *AFT1*-independent pattern of iron regulation and not to contain an *AFT1* consensus binding site (13), our results show that *ARN3* is iron- and *AFT1*-regulated. Transcriptional regulation by *AFT1* was confirmed by Northern analysis, and inspection of upstream sequences indicate an Aft1p consensus binding site for each of the *ARN* genes (12, 31). The *ARN* genes were grouped as members of the major facilitator superfamily of transporters on the basis of their predicted amino acid sequences (25–27). Walker A and Walker B motifs are absent, indicating that these potential permeases are not ATP-binding cassette-type transporters and likely require proton symport to energize the transport of substrate. Members of this gene family have 12–14 membrane-spanning domains and function as uniporters, symporters, and antiporters of a variety of small molecules, including drugs, sugars, and amino acids. The *ARN* genes are predicted to have 14 transmembrane domains, a less common feature of the major facilitator superfamily transporters that is shared by the multidrug proton antiporter subfamily. Interestingly, these two subfamilies also transport the largest substrates of any of the major facilitator superfamily subfamilies, as siderophores are approximately 500–1000 M_r and the larger drugs 400–500 M_r .

Very little is known about siderophore uptake in eukaryotes, although the process has been studied in detail in prokaryotes (7). In the *E. coli* K-12 strain, a single siderophore, enterobactin, is synthesized and secreted, whereas six different iron-siderophore uptake systems have been identified, each one specific for a different siderophore. The sequence and predicted structure of the ARN family of transporters, however, do not resemble those of prokaryotic siderophore transporters; presumably eukaryotes have evolved distinct mechanisms for siderophore-mediated iron uptake. The fungus *Ustilago maydis* exhibits two different pathways of siderophore-mediated iron uptake (32, 33). The native siderophore ferrichrome enters the cell as an iron chelate and over time accumulates in vesicles in the iron-free form. Xenosiderophores, such as ferrioxamine B, as well as the native siderophore ferrichrome A, do not cross

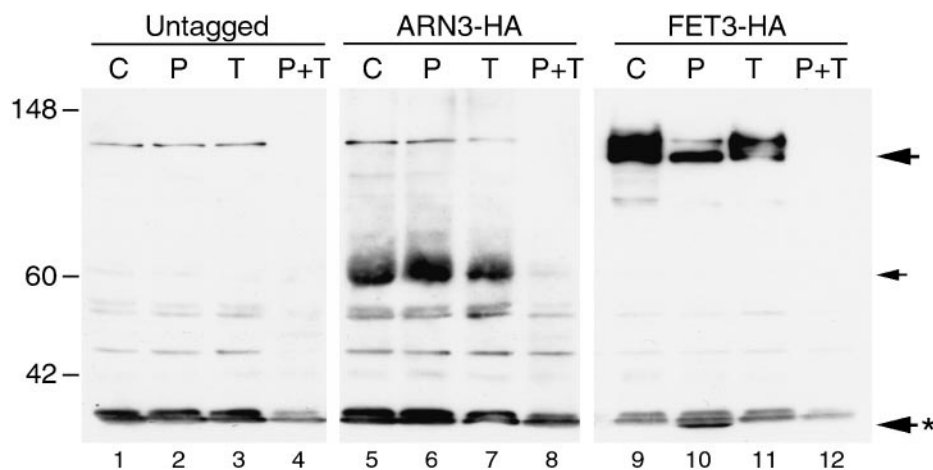


FIG. 6. **Resistance of Arn3p-HA to extracellular proteases.** Congenic strains expressing the wild type level of Arn3p-HA or overexpressing Fet3p-HA and the untagged parent strain were grown in YPD media to exponential phase. Cells were then incubated with buffer alone (C), with Pronase (P), with Triton (T), or Pronase and Triton (P+T) on ice for 1 h prior to lysis. Lysates were analyzed by SDS-polyacrylamide gel electrophoresis and Western blotting. Intact Arn3p-HA (small arrowhead), intact Fet3p-HA (large arrowhead), and the Fet3p-HA proteolytic fragment (large arrowhead, starred) are indicated. Molecular masses in kDa are indicated on the left. Results did not differ when cells were incubated with proteinase K for 20 min instead of Pronase.

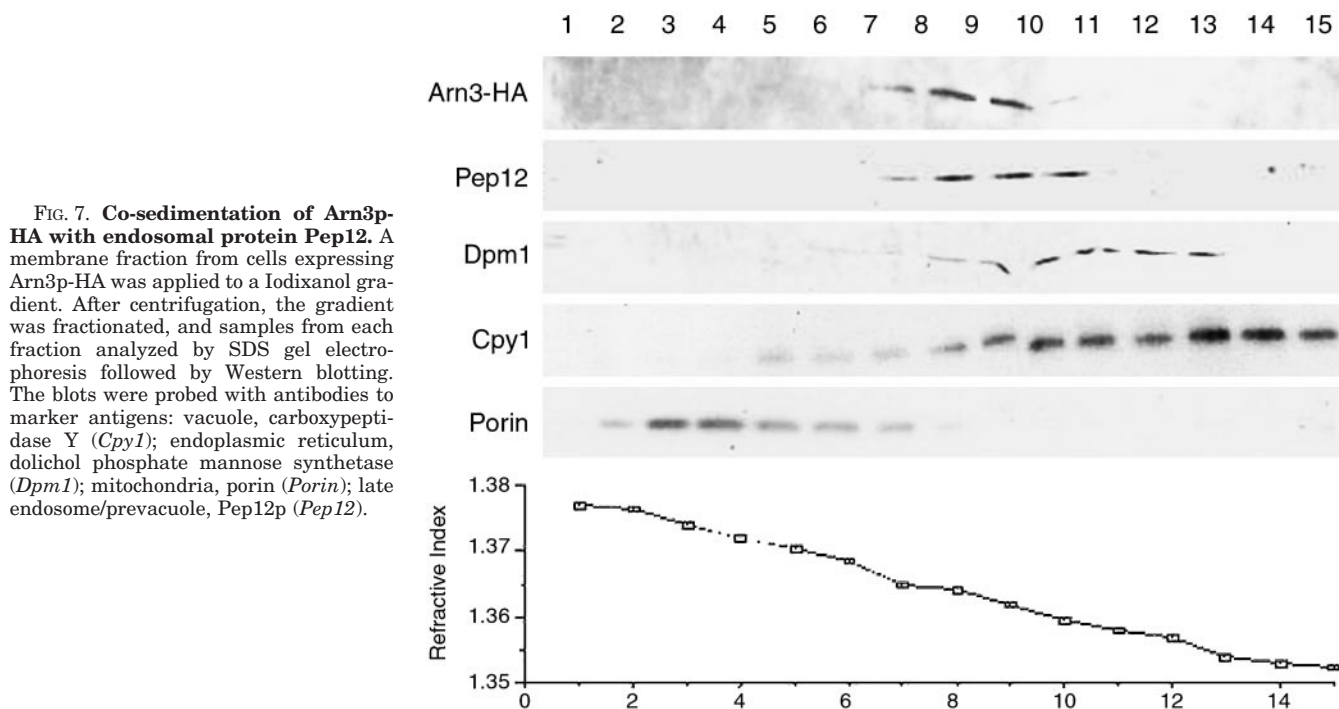


FIG. 7. **Co-sedimentation of Arn3p-HA with endosomal protein Pep12.** A membrane fraction from cells expressing Arn3p-HA was applied to a Iodixanol gradient. After centrifugation, the gradient was fractionated, and samples from each fraction analyzed by SDS gel electrophoresis followed by Western blotting. The blots were probed with antibodies to marker antigens: vacuole, carboxypeptidase Y (*Cpy1*); endoplasmic reticulum, dolichol phosphate mannose synthetase (*Dpm1*); mitochondria, porin (*Porin*); late endosome/prevacuole, Pep12p (*Pep12*).

the plasma membrane but are bound at the cell surface where the iron is reduced extracellularly before entering the cell. The capacity of microbes to take up iron from siderophores that are secreted by other species appears to be well conserved and likely provides a selective advantage in a natural environment where many species compete for nutrients.

Our studies indicate that *S. cerevisiae* has two different systems of DFO-mediated iron transport: one that requires the *FET3*-dependent, high affinity, iron transport system and a second that requires *ARN3*. In the first system, DFO-Fe could act as a substrate for surface reductases, releasing Fe(II), which is then taken up by the high affinity iron transport system. This transport system is independent of the *ARN* genes. The second transport system for DFO-Fe only becomes apparent in the absence of Fet3p. This transport system is specific for *ARN3*; deletion of the other highly homologous *ARN* genes either singly or in combination does not lead to a defect in DFO-Fe transport.

Our finding that Arn3p (and other *ARN* family members; data not shown) is primarily localized to endosome-like vesicles indicates that *ARN3*-dependent uptake differs from *FET3*-dependent uptake. Arn3p was localized by immunofluorescence and biochemical techniques to intracellular vesicles. Although our data cannot exclude the possibility that a small amount of Arn3p localized to the cell surface, it clearly shows that the bulk of the protein is present in an intracellular organelle. This result suggests two possibilities: 1) that Arn3p localizes briefly to the cell surface, where it facilitates DFO-Fe transport, before being internalized or 2) that DFO-Fe is delivered to Arn3p in an intracellular, metal-exchanging compartment. The entry of DFO-Fe could occur by fluid phase endocytosis, or alternatively, DFO-Fe chelates may be recognized by specific binding proteins at the plasma membrane, which are then internalized. In either case, the site of iron release may be the intracellular vesicle. A precedent for this system of intravesicular iron release occurs in mammalian transferrin-dependent iron uptake

(34). In this system, the "siderophore" is transferrin, which binds with high affinity to Fe(III) in the extracellular fluid. Diferric transferrin then binds to the transferrin receptor on the plasma membrane, and the complex is internalized via receptor-mediated endocytosis. Iron is released from transferrin within the endocytic vesicle and reduced, Fe(II) is transported across the endosomal membrane by the permease DMT1. If siderophore-iron uptake in budding yeast is similar to transferrin-iron uptake in mammalian cells, then a testable prediction is that an intracellular ferrireductase may exist. Studies that test this prediction are in progress.

Acknowledgments—We thank Robert Stearman and Richard Klausner for the gift of plasmids.

REFERENCES

- Dix, D. R., Bridgham, J. T., Broderius, M. A., Byersdorfer, C. A., and Eide, D. J. (1994) *J. Biol. Chem.* **269**, 26092–26099
- Askwith, C., Eide, D., Van Ho, A., Bernard, P. S., Li, L., Davis-Kaplan, S., Sipe, D. M., and Kaplan, J. (1994) *Cell* **76**, 403–410
- Stearman, R., Yuan, D. S., Yamaguchi-Iwai, Y., Klausner, R. D., and Dancis, A. (1996) *Science* **271**, 1552–1557
- Dancis, A., Klausner, R. D., Hinnebusch, A. G., and Barriocanal, J. G. (1990) *Mol. Cell. Biol.* **10**, 2294–2301
- Georgatsou, E., and Alexandraki, D. (1994) *Mol. Cell. Biol.* **14**, 3065–3073
- Byers, B. R., and Arceneaux, J. E. L. (1998) in *Iron Transport and Storage in Microorganisms, Plants, and Animals* (Sigel, A., and Sigel, H., eds) Vol. 35, pp. 37–66, Marcel Dekker, New York
- Braun, V., Hantke, K., and Koster, W. (1998) *Met. Ions Biol. Syst.* **35**, 67–145
- Leong, S. A., and Winkelmann, G. (1998) in *Iron Transport and Storage in Microorganisms, Plants, and Animals* (Sigel, A., and Sigel, H., eds) Vol. 35, pp. 147–186, Marcel Dekker, New York
- Neilands, J. B. (1995) *J. Biol. Chem.* **270**, 26723–26726
- Lesuisse, E., Raguzzi, F., and Crichton, R. R. (1987) *J. Gen. Microbiol.* **133**, 3229–3236
- Yamaguchi-Iwai, Y., Dancis, A., and Klausner, R. D. (1995) *EMBO J.* **14**, 1231–1239
- Yamaguchi-Iwai, Y., Stearman, R., Dancis, A., and Klausner, R. D. (1996) *EMBO J.* **15**, 3377–3384
- Lesuisse, E., Simon-Casteras, M., and Labbe, P. (1998) *Microbiology* **144**, 3455–3462
- Albrect-Gary, A., and Crumbliss, A. L. (1998) in *Iron Transport and Storage in Microorganisms, Plants, and Animals* (Sigel, A., and Sigel, H., eds) Vol. 35, pp. 239–328, Marcel Dekker, New York
- Philpott, C. C., Rashford, J., Yamaguchi-Iwai, Y., Rouault, T. A., Dancis, A., and Klausner, R. D. (1998) *EMBO J.* **17**, 5026–5036
- Schneider, B. L., Steiner, B., Seufert, W., and Futcher, A. B. (1996) *Yeast* **12**, 129–134
- Stearman, R., Dancis, A., and Klausner, R. D. (1998) *Gene (Amst.)* **212**, 197–202
- Schneider, B. L., Seufert, W., Steiner, B., Yang, Q. H., and Futcher, A. B. (1995) *Yeast* **11**, 1265–1274
- Sherman, F. (1991) in *Guide to Yeast Genetics and Molecular Biology* (Guthrie, C., and Fink, G., eds) Vol. 194, pp. 3–20, Academic Press, New York
- DeRisi, J. L., Iyer, V. R., and Brown, P. O. (1997) *Science* **278**, 680–686
- Spellman, P. T., Sherlock, G., Zhang, M. Q., Iyer, V. R., Anders, K., Eisen, M. B., Brown, P. O., Botstein, D., and Futcher, B. (1998) *Mol. Cell* **9**, 3273–3297
- Dancis, A., Yuan, D. S., Haile, D., Askwith, C., Elde, D., Moehle, C., Kaplan, J., and Klausner, R. D. (1994) *Cell* **76**, 393–402
- Nothwehr, S. F., Conibear, E., and Stevens, T. H. (1995) *J. Cell Biol.* **129**, 35–46
- Radisky, D. C., Babcock, M. C., and Kaplan, J. (1999) *J. Biol. Chem.* **274**, 4497–4499
- Pao, S. S., Paulsen, I. T., and Saier, M. H., Jr. (1998) *Microbiol. Mol. Biol. Rev.* **62**, 1–34
- Nelissen, B., De Wachter, R., and Goffeau, A. (1997) *FEMS Microbiol. Rev.* **21**, 113–134
- Goffeau, A., Park, J., Paulsen, I. T., Jonniaux, J. L., Dinh, T., Mordant, P., and Saier, M. H., Jr. (1997) *Yeast* **13**, 43–54
- Askwith, C. C., and Kaplan, J. (1998) *J. Biol. Chem.* **273**, 22415–22419
- De Silva, D. M., Askwith, C. C., Eide, D., and Kaplan, J. (1995) *J. Biol. Chem.* **270**, 1098–1101
- Becherer, K. A., Rieder, S. E., Emr, S. D., and Jones, E. W. (1996) *Mol. Biol. Cell* **7**, 579–594
- Lin, S. J., Pufahl, R. A., Dancis, A., O'Halloran, T. V., and Culotta, V. C. (1997) *J. Biol. Chem.* **272**, 9215–9220
- Ardon, O., Weizman, H., Libman, J., Shanzer, A., Chen, Y., and Hadar, Y. (1997) *Microbiology* **143**, 3625–3631
- Ardon, O., Nudelman, R., Caris, C., Libman, J., Shanzer, A., Chen, Y., and Hadar, Y. (1998) *J. Bacteriol.* **180**, 2021–2026
- Aisen, P. (1998) *Met. Ions Biol. Syst.* **35**, 585–631